

Multiscale Physical Characterization of Subglacial Sediments from the 1966 Camp Century Core

A Thesis Proposal Presented

by

Cat Collins

to

Rubenstein School of Natural Resources and the Environment

at

The University of Vermont

December 2023

Submitted to the Faculty of the Rubenstein School of Natural Resources and the Environment,
the University of Vermont, in partial fulfillment of the requirements for the degree of Master of
Science specializing in Natural Resources.

The following are members of this Thesis Committee:

Paul Bierman, PhD, Advisor

Nicolas Perdrial, PhD

Donna Rizzo, PhD

Abstract

The stability of the Greenland Ice Sheet (GrIS) in a warming climate is a major concern for the viability and safety of coastal cities. The key to understanding the future of GrIS melt and sea-level rise contributions is stored in its past. It is typical for polar scientists to study Greenland's paleoclimate using ice core analyses. Now we have unique access to 3.44 meters of frozen sediment from the bottom of the Camp Century ice core. Studying basal sediment from ice sheets can give unique insight into ice-sheet processes at the base, the timing of prior ice-free events, and information about depositional environments that cannot be gained with ice-core analyses. Deciphering what environments and mechanisms deposited this sediment and what evidence there is of post depositional processes is crucial for understanding conditions at time of deposition and will expand our understanding of Greenland's climate history.

I used 26 samples for this study. Analytical techniques I used include micro-computed tomography (μ CT), x-ray diffraction (XRD), and scanning electron microscopy (SEM) to understand the contents of the core and what surface processes are recorded in the sediments. From evaluation of the scans and sedimentological observations, I defined 5 distinct stratigraphic units within the core. XRD analysis so far reveals that the quartz dominates the mineralogy and feldspar throughout each unit with minimal variability. SEM analysis shows that in the lower units there are extensive clay-size grain coatings that are absent in the upper layers.

My work to date shows evidence of a glaciated Greenland followed by a period of ice-free conditions. The lower diamicton (unit 1) is likely a glacial till that records a time when ice was present at the coring site. The intermediate ice layer (unit 2) remains of uncertain origin but it could be a permafrost ice wedge or basal ice. Unit 3 could be a slump deposit, indicated by disturbed bedforms and poor sorting. It could also be entrained sediment in the basal ice due to its similarity with unit 1. The upper 2 units are sandy deposits likely transported by fluvial processes and represent the absence of ice. Unit 4 is laden with fine sediment indicating deposition from a low energy environment. The uppermost unit (unit 5) shows upward coarsening that likely indicates a higher and more variable energetic environment than unit 4, possibly a meandering stream.

The μ CT scans provide high resolution 3-dimensional models of the sub-glacial sediment core. The preservation of the original depositional forms allows for intricate insight into the surface processes at the time of original deposition. The creation of this digital archive optimizes data collection as destructive analysis of the physical sediment for other multiproxy analysis can occur in tandem. Deciphering the sedimentary history using these multiscale methods provides evidence of Greenland's ice-free past. As the GrIS continues to melt, we can use information of its stability in past warm climates to inform climate models and notify the public, policy makers, and those exposed to high flood risk what to expect in the near and distant future.

Introduction

The Arctic is warming at a faster rate than any other region on Earth (Manabe & Stouffer, 1980). Arctic amplification, characterized by increased temperature in high latitude regions, ranges from 1.5 to 4 times global mean temperatures (Rantanen et al., 2022). Specific feedback loops, like the ice-albedo interaction, during which melting of the highly reflective ice leaves behind darker areas of ocean and land that absorb more incoming solar energy, drive the amplified warming (Manabe & Stouffer, 1980). Unsurprisingly, Greenland is losing ice mass at an increased rate due to this sustained elevated temperature (Smith et al., 2020). This is concerning because mass loss (melt) from Greenland's ice sheet alone could lead to more than 7 meters of sea-level rise. If we continue with the current rate of carbon

emissions, ice sheet mass loss and subsequent sea-level rise will threaten the viability of coastal cities and nations (Dutton et al., 2015), potentially affecting the 1.81 billion people exposed to high flood risk (Rentschler et al., 2022).

The key to understanding the future of Greenland melt lies in records of past ice-free events. The Pleistocene, the geologic epoch that occurred between 2.58 million to 11,700 years ago, is the most recent time in history when Earth experienced repeated glaciations and deglaciations. Referred as Marine Isotope Stages (MIS), these glacial and interglacial periods provide useful analogues for times when Earth's atmosphere was as warm or warmer than it is now (Lisiecki & Raymo, 2005). Scientists often look to MIS 5e (119 to 127 ka) and MIS 11 (374 to 424 ka) as analogues for the future of Greenland ice sheet (GrIS) melt and contribution to sea-level rise. This is because both had similar CO₂ concentrations to the pre-industrial era but had slightly higher global average temperatures (Kukla et al., 1997; Loutre & Berger, 2003).

During MIS 5e, the last interglacial, atmospheric CO₂ peaked at a concentration similar to preindustrial levels (Lüthi et al., 2008) and sea level at that time is estimated to have been 6-9 m above modern levels (Dutton et al., 2015). Though global temperature was about 2°C warmer than today, studies show that the GrIS shrank minimally (Bender et al., 2010; Johnsen et al., 2001; Suwa et al., 2006; Svensson et al., 2011; Willerslev, Cappellini, Boomsma, Nielsen, Hebsgaard, Brand, Hofreiter, Bunce, Poinar, Dahl-Jensen, Johnsen, Steffensen, Bennike, Schwenninger, Nathan, Armitage, De Hoog, et al., 2007; Yau et al., 2016).

MIS 11 was the longest and warmest interglacial during the Pleistocene. Global average temperature during this time is uncertain but most estimates suggest temperatures up to 2°C higher than pre-industrial levels (Dutton et al., 2015; Jouzel et al., 2007). Atmospheric CO₂ peaked at 286 ppm, again similar to preindustrial levels (Lüthi et al., 2008), and the sea level was 6 to 13 meters above modern levels due to GrIS, mountain glaciers, and Antarctic mass loss (Dutton et al., 2015). Pollen studies indicate the development of a boreal coniferous forest in southern Greenland which would require the ice to fully retreat from the region (Reyes et al., 2014; de Vernal & Hillaire-Marcel, 2008). Other studies focused on MIS 11 suggest southern GrIS collapse (Reyes et al., 2014b), northwestern GrIS retreat (Christ et al., 2023), but persistence of the ice sheet in the eastern highlands (Bierman et al., 2016). All scenarios, though, indicate a smaller GrIS extent and subsequent sea-level rise.

Two common methods used to infer the climate of the Pleistocene are based on ice cores and marine cores of ice rafted debris. With ice cores scientists often study ancient atmosphere trapped in bubbles in the ice, water isotopes, and volcanic tephra to name a few methods. Marine cores utilize the presence of ice-rafted debris which are materials transported by icebergs that deposit on the ocean floor when the ice melts (Bond et al., 1992; Grousset et al., 1993; Johnsen et al., 2001; Lisiecki & Raymo, 2005). A caveat of these methods is that both necessitate the presence of ice in the past. When the ice was gone, we cannot use these methods as easily to understand paleoclimate. In this case, preserved sediment beneath the ice can reveal crucial information about ice-free events, their duration, and specific surface processes that occurred with in-situ physical evidence to expand our understanding of Greenland's paleoclimate that is not recorded in ice (Bierman et al., 2014; Christ et al., 2021, 2023).

Basal material pulled from the bottom of the GrIS has received less attention than the ice cores since the various drilling projects ended. Of the drilling projects Camp Century, NEEM, GRIP, GISP2, and Dye-3 retrieved either basal material or silty ice (Blard et al., 2023; Christ et al., 2021; Gow & Meese, 1996; Souchez et al., 1994, 1998; Willerslev, Cappellini, Boomsma, Nielsen, Hebsgaard, Brand, Hofreiter, Bunce, Poinar, Dahl-Jensen, Johnsen, Steffensen, Bennike, Schwenninger, Nathan, Armitage,

De Hoog, et al., 2007). Of all of these, the Camp Century subglacial sediment core is the most substantial, containing 3.44 meters of basal materials (Hansen & Langway, 1966b). This sediment core is made up of several units, the deepest being older than 1 million years old. Data show the top portion was last at the surface 416,000 years ago, which places it during MIS 11 (Christ et al., 2021, 2023). From this core we can gather information about past environmental processes and sea-level rise which can aid in our understanding of the more recent interglacials.

Objectives

My thesis investigates the stratigraphy and mineralogy of the core sediments to support and inform other studies investigating this same core. Understanding the physical makeup of the Camp Century basal sediments can lead to a detailed interpretation of the origins of the sediments. This thesis is integral to a joint effort to reconstruct the paleoclimate at the Camp Century drill site in Greenland 400,000 years ago and beyond. In addition to understanding the past climate we will also be able to understand past surface processes in a glaciated and deglaciated Greenland as well as post depositional processes.

My objective is to use mineralogic and stratigraphic analysis on the Camp Century subglacial sediment core to extract information about the evolution of environmental conditions and landscapes during the last ice-free event in NW Greenland.

I will use multiscale analysis to elucidate processes that happened during deposition and have been recorded in the sediments, to reconstruct Greenland's environmental conditions during MIS 11 and further back in time.

Background

History and prior works

Camp Century

Camp Century was located in Northwestern Greenland, ~200 km inland from the ice margin. The creation of this camp was one of the US responses to Russian threat during the Cold War (Clark, 1965). The US military chose this location because Greenland was the shortest distance between these two major nuclear powers (Clark, 1965). Out of fear of Russian threat, the US moved to militarize the arctic. In parallel to (and potentially as a cover for) the military efforts, the army core of engineers built an arctic research center, operated by personnel from the Snow, Ice and Permafrost Research Establishment (SIPRE), now known as the Cold Regions Research and Engineering Lab (CRREL) (Langway, 2008). At this camp, the Army drilled the first deep ice core and the largest archive of subglacial sediment that exists to date (Langway, 2008). The ice from this core was studied extensively (e.g., Hansen & Langway, 1966a; Johnsen et al., 1972; Langway & Hansen, 1970; W. Dansgaard et al., 1969) but the sediment was left relatively untouched save for a handful of studies (Fountain et al., 1981; Harwood, 1986; Whalley & Langway, 1980). The sediment then disappeared until the late 2010s where its rediscovery in the Niels Bohr Institute at the University of Copenhagen sparked new interest in analyzing this deep sediment archive.

Past works

Subglacial material from beneath the ice is a valuable source of paleoclimate information (Bierman et al., 2014; Finkel & Nishiizumi, 1997). From GrIS deep ice core archives, there are debris-rich basal sections in Camp Century, GISP2, and NEEM and a minimal amount from Dye-3 and GRIP (Tison et al., 2019). This "silty ice" was the focus for past investigations on ice-flow properties and basal-ice deformation

(Bender et al., 2010; Gow & Meese, 1996; Souchez et al., 1998; Souchez, Lemmens, et al., 1995). Additionally, other studies leveraged stable isotopes to understand the original formation of the ice sheet including the paleoenvironment present as the ice sheet accumulated (Souchez et al., 1994, 2006; Souchez, Janssens, et al., 1995). These studies focused more on the properties that we can learn from ice instead of the sediment in the ice.

Prior studies that have investigated the sediments in the basal ice did so with the objective of understanding ice sheet stability. Even with the limited material, some scientists have found evidence from pollen proxy records at Dye-3 and from marine cores that the ice sheet retreated in the southern region during MIS11 (de Vernal & Hillaire-Marcel, 2008; Willerslev et al., 2007). Others reported evidence of extended periods of ice retreat during the Pleistocene but did not constrain the exact timing and length of these deglaciations (Bierman et al., 2016; Schaefer et al., 2016). The renewed interest in basal sediments from the rediscovery of the Camp Century archive has led to more studies with this same objective. Evidence from the archive has led to the conclusion that Greenland melted more substantially than previously believed, leaving Camp Century completely ice-free, 416,000 +/- 38,00 years ago (MIS11) (Christ et al., 2021, 2023). Expanding on the constraints identified in the Camp Century sediment, another study uses a multiproxy approach to understand the nature of the basal ice layer of the NEEM core (Blard et al., 2023). Blard et al. hypothesize a similar sequence for glacial retreat and advance as identified in the Camp Century sediments (Blard et al., 2023). More in-depth analysis on the Camp Century sediment archive will further expand our understanding of the paleoenvironment when the ice retreated, the mechanisms of glacial and subaerial processes, and can help us refine our understanding of ice retreat and advance sequencing.

Stratigraphic analysis on subglacial sediment

The Camp Century sediments are so well preserved that we can employ standard geologic practices to study the stratigraphy and mineralogy. The high degree of preservation allows us to study the sediment with a high degree of detail irrespective of the deglaciation that covered them in a mile of ice. The most basic and key example of what methods we can employ is observational sequence stratigraphy and identification of facies within sedimentary units. In understanding these elements, we can infer what paleo-environments were present when this sediment package was deposited.

Diagnostic features:

Fluvial sediments

Fluvial sediment deposits form by the transport and deposition of sediment by flowing water. There is a great diversity of fluvial sediments across the globe. Detailed observation of the sediment units in context of the morphology of the landscape can lead to interpretations of specific depositional environments. In a fluvial environment, these features are determined by the source rock and the energy of the system (Johnson, 1981). Typically, sedimentological analysis focuses on grain size, angularity, sorting, and orientation to determine the characteristics of the depositional environment. These features can be indicators of maturity and travel distance from the source material (Johnson, 1981). A mature sediment will be well sorted, meaning the grain size distribution is uniform, and the grains will be highly rounded. An additional indication can be the type of minerals included since different mineral weather at different rates. For example, as quartz is highly resistant to weathering, sediments with high quartz percentages are more mature, though this can be context specific. A sediment with a higher degree of sorting indicates a larger distance from the source, the size of the grain is dependent on a positive correlation with the system energy, and angularity is negatively correlated with system energy and transport distance (Johnson, 1981).

Diamicton and glacial till

Diamictons are sedimentary formations characterized by rock fragments of highly variable sizes supported by a matrix of sand to fine-grained sediments (Young, 2016). These can be associated with glacial activity in which case we often refer to them using the genetic term “glacial till”. The glacier or ice sheet forms the till as it moves across and erodes the landscape beneath it. Till can accumulate at the front and sides of the glacier in which case we refer to it as a moraine, but it can also stay beneath the ice body in which case it is subglacial till (Evans et al., 2006).

Basal ice

Basal ice is distinct from typical glacier ice as it is subject to active processes at the ice-bed interface. Glaciers form by firnification which describes a compression of snow as it accumulates year after year. Basal ice is at great depth where there is immense pressure that can cause deformation and melting. The thickness of this layer is usually much larger when the glacier is cold based, meaning it experiences less pressure-driven melting. Debris at the ice-bed interface also commonly gets entrained in the basal ice as it experiences this strain (Knight, 1997). Distinct structures that result from this entrainment can vary from “discrete bands, sets of fine laminations, and apparent suspensions of dispersed particles or particle aggregates” (Knight, 1997). This can look like portions of ice with small, suspended clasts, or it can lead to multi-centimeter thick bands of sediment inserted in the ice. Previous studies also identified deformation structures from comparing the GRIP and GISP2 cores (Grootes et al., 1993; Taylor et al., 1993). The features of basal ice are very distinct from glacier ice which has less sediment impurities and has horizontal annual layering which gets overprinted and erased in basal ice.

Permafrost and segregation ice

Permafrost is frozen earth surficial material that stays frozen for more than 2 years (French & Shur, 2010). The upper portion of permafrost can experience melting annually, in which case this upper portion is the “active layer.” A common way to study permafrost is by close inspection of cryostructures, which are ice structures that occur in frozen sediment. Ground ice is a component of cryostratigraphy and consist of three important types: pore ice, segregation ice, and ice lenses. Pore ice is the water in the sediment deposit that froze originally (French & Shur, 2010). Segregation ice forms when unfrozen water moves toward the freezing plane (the boundary between conditions supporting liquid water versus frozen water, or the 0°C isotherm) and aggregates, sometimes forming up to tens of meters thick ground ice. Ice lenses form in an analogous way but are much smaller often just a few millimeters thick but can be highly abundant (French & Shur, 2010). They can also have a consistent inclination which reflects the orientation of the freezing plane (French & Shur, 2010). It important to note that ground ice can also include buried ice which formed from external processes (Murton & French, 1994). Identifying sediment stratigraphy from cryostructures alone can be difficult so it is common to use geochemistry of the waters to identify original depositional conditions (Meyer et al., 2002).

Micro-scale Grain Features

Grain coatings and microtextures are examples of micro-scale records of environmental, depositional, and post-depositional processes (Mahaney, 2011; Schindler & Singer, 2017). Grain coatings can form from the precipitation of elements sourced from either grain dissolution or fluids in the surrounding sediments (Schindler & Singer, 2017). In a glacial context, this can happen from in-situ weathering, or it is common to see an agglomeration of variably sized grains adhered by rock flour (fine particles, $<63\mu\text{m}$, formed during glacial abrasion) (Benn, 2009). This could indicate either a paleosol (ancient soil) or an active glacial environment, respectively (Blard et al., 2023). The absence of grain coatings can also be valuable information as we would know that it would be less likely the sample came from a paleosol or a glacial deposit. Microtextures can give us similar information as the grain textures reflect their transport mechanisms. Microtextures are common among sediments from various transport mechanisms. Some examples are the fracture face, conchoidal fractures, arc-shaped steps, etc. (Mahaney, 2011). Microstriations, though, are diagnostic of glacial transport and can only be formed by the intense physical weathering that a glacier provides (Mahaney, 2011).

Sediment Mineralogy

Sediment mineralogy can be an important indicator of sediment source and post depositional transformations. Identification of source change hinges on observations of changes in the relative abundance of mineral assemblages throughout the sediment column. Any abrupt, significant alteration in relative abundance or mineral type could be an indication a source change. Due to limited knowledge of subice Greenland bedrock geology (fig 1) only a general understanding of source change is achievable. If source change was evident, it could point to variation of the ice flow direction as that is the main source of erosion in northwestern Greenland.

Post depositional processes can be a cause for more subtle changes in mineralogy. An example of an in-situ process is pedogenesis, the formation of soil by means of physical and chemical weathering. Weathering breaks down existing material into smaller and smaller pieces and creates clay- and silt-sized particles. Concomitantly, it breaks down the parent material with a variety of chemical reactions that alter its original composition. During soil formation in igneous rocks pyroxenes and hornblendes weather first (Johnson, 1981). During this process biotite weathers into vermiculite and oligoclase and microcline both tend to decrease in abundance (Johnson, 1981). These are replaced by clay minerals, so a higher degree of weathering is typically indicated by an increase in clay abundance (Velde, 1995). In addition, quartz is a very stable mineral, so it appears in high relative abundance in weathered rocks.



Figure 1 Geological map of Greenland from Dawes et al., 2009

Methods

Core cutting procedure and sample allocations

The core cutting procedure was done in a cold room at the Ice Core Facility of the Centre for Ice and Climate, NBI, at the University of Copenhagen, Denmark. Given the expansive network of scientists involved in this work, we based the cutting procedure on sample allocation for the various analyses that our collaborators will conduct. In the context of this study, I utilized subsamples (a) and (b), the long peripheral pieces, for my analyses (fig 2). I processed these subsamples both while they were frozen and after thawing them. I used the frozen samples for micro computed tomography (μ CT). After thawing the subsamples, they were processed for pore water, bulk biologic material, and bulk sediment analyses. I used the bulk sediment for X-ray diffraction analysis (XRD), and scanning electron microscopy (SEM) analysis.

Micro-Computed Tomography

I collected μ CT scans to create a digital record of the (a) and (b) sub-samples and to measure sedimentological properties (porosity, grain size and grain shape) at micron (μ m) scale resolution (fig 2). I scanned sub-samples (a) and (b) from each sample using a Bruker SkyScan 1173 μ CT scanner fit for use in a cold room at -10°C at the CRREL in Hanover, NH (fig 2). I scanned full-sized, ~ 10 cm-tall samples in two overlapping 7.9 cm-tall sections at a resolution of $71 \mu\text{m}/\text{pixel}$ for the bottom (BOT) and the top (TOP) of the sample. This captured the entire length of the sample over the two scans. I complete reconstructions for each scan using the Bruker NRecon software. This resulted in 100 partial sample scans, 4 full sample scans, and 8 zoomed scans with two failed reconstructions due to difficulty in the scanning procedure.

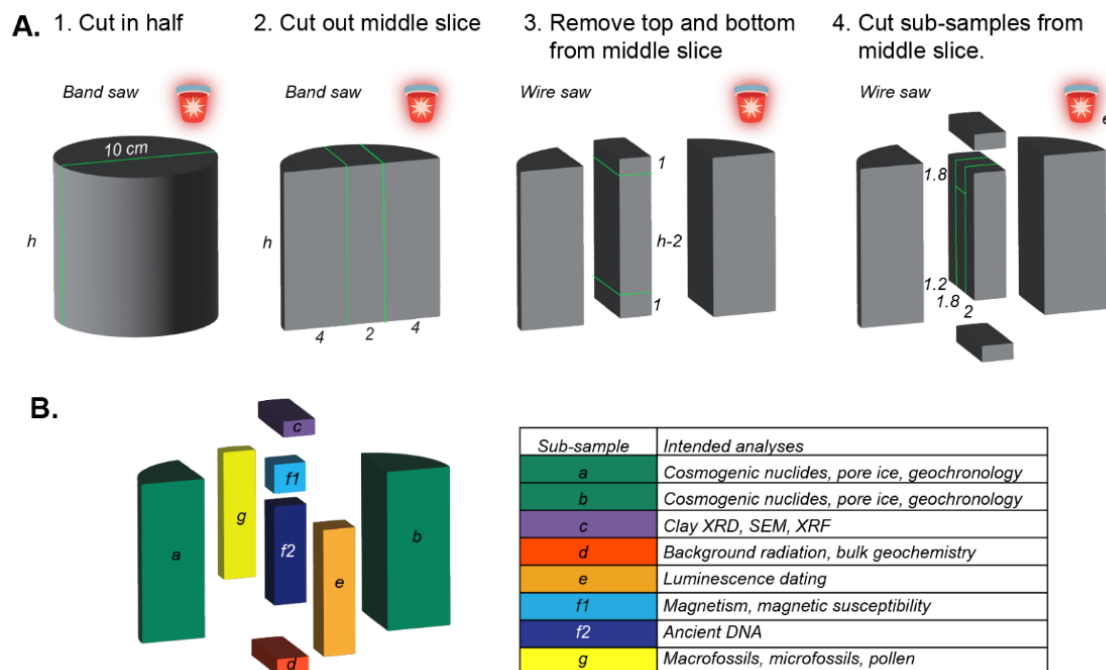


Figure 2 (A) Core cutting procedure conducted under redlight conditions for each sample of the Camp Century archive. We cut each subsample based on required material for analysis technique. We imaged subsets a and b before we melted them for other analyses like cosmogenic nuclide, pore ice geochemistry, or other palaeoecological work. (B) proposed usage for each subsample based on analysis type and material requirements.

With full 3D models, is it easier to identify sediment structures in the samples which will aid in our environmental interpretations. The creation of one full scan from the two halves requires post-production processing includes using the *Stitching* FIJI plugin (Schindelin et al., 2012), which utilizes a globally optimal stitching algorithm to match the overlapping sections for the 40 samples that required it (Preibisch et al., 2009). To do this, I created image stacks in .tiff format for each TOP and BOT scans using FIJI stack options. In this step, it was important to establish a relevant volume of interest (VOI) using the software CTan (Bruker) with the same dimensions for the TOP and BOT scan before attempting to stitch. Not doing this resulted often in a misregistration of the two scans in 3D space and the subsequent stitched sample did not replicate the original sample geometry. Once ensuring this, I opened the *Stitching* plugin and, using Grid stitching and specifying sequential images, used a linear blending fusion method. After the algorithm registered each image in 3D space and aligned to overlapping sections (~40 minutes), I saved the fusion as an image sequence in .tiff format. I then made a new VOI of the fusion in CTan and used that VOI in CTvox (Bruker) to assess the validity of the *Stitching* output. This methodology worked for 39 of the 40 subsamples with overlapping scans.

X-ray Diffraction

I completed a quantitative XRD analysis of selected core samples using a Rigaku MiniFlex II, equipped with a Cu X-ray tube. Quantitative XRD can tell us the relative distribution of crystalline material in each sample. Variations in the distribution can clue us in to pre-, syn-, and post-depositional processes (evidence of source change, transport fractionation and weathering). This analysis surveyed 16 samples. We made sure to select a representative spread of samples by ensuring we had samples from each hypothesized unit and ones near contacts (Table 1). I used bulk sediment taken from the core for each unit and ground it manually with a mortar and pestle. Because the amount of material was limited, I mounted the ground sediments on a zero-background plate in random orientation mounts. I analyzed the samples in 2theta-theta geometry between 3 and 70 °2θ with a dwell time of 1 degree/min and 0.02 °2θ resolution for a total 67-minute run time. I analyzed diffractograms qualitatively using a database from the International Center for Diffraction Data 2.0 and Crystallography Open Database for peak matching. I performed quantitative analysis of the X-ray diffractograms using a semi-automatic Rietveld approach (Rietveld, 1969) in the whole pattern profile fitting module of the PDXL-2 software. To refine our results, I varied the values for scale factor, cell parameters (within 0.2Å), shape parameters, and for selected minerals (clays and amphiboles) the preferred orientation March–Dollase parameter.

Scanning Electron Microscopy Imaging and Energy Dispersive X-ray micromapping

For SEM analysis, I embedded the thawed selected bulk sediments taken from subsamples (a) and (b) (Table 1) in epoxy (EPO-TEK 301). After curing for at least 24 hours, I grinded and micropolished the epoxy puck using a decreasing grit size to 0.05 μm. The pucks were carbon sputter-coated prior to analysis in backscattered electron (BSE) mode using a TESCAN VEGA3 scanning electron microscope coupled with an Oxford Instruments AZtec Elemental Mapping EDS in the Geology Department at Middlebury College. I acquired BSE images and energy dispersive x-ray spectrometry (EDS) maps at 20 keV for a minimum of 20 frames totaling 10-minute elapsed time for each multi-elemental map. Then I generated multi and tri-color maps using the Gatan digital micrograph 3.1 software.

I postprocessed the EDS maps to analyze grain size and grain shape parameters using Fiji (Schindelin et al., 2012). Using the color-coded maps of Si-Al-Fe distribution, I performed a color threshold to select the Si-O phases only (quartz). I then set the scale parameters and cleaned the background noise before performing a particle analysis to return the size, circularity, and roundness of the quartz grains. Circularity is a measure (between 0 and 1) of the shape of the grain, and ranges from elongated (0) to perfectly

circular (1); Roundness is a measure (between 0 and 1) of the roughness of the grain, and ranges from rough (0) to smooth (1). When applied to quartz grains, both parameters inform syn- and post-depositional processes such as surface alteration during transport or aeolian erosion.

Table 1 Samples used in SEM and XRD analysis, their unit, and proximity to the contact between units. In the case of limited available material, I performed only one analysis type. This only occurred for sample 1060-C4 and 1061-A. Cells marked red indicate that analysis type was not completed. Samples names are color coded according to their unit number.

Core Tube	Sample	Unit	XRD	SEM	Proximity to Contact
1059	CC1059-5	5			
	CC1059-6	5			Above contact
	CC1059-7	4			Under contact
1060	CC1060-A2	4			
	CC1060-B	4			Above contact
	CC1060-C1	3			Under contact
	CC1060-C2	3			
	CC1060-C4	2	Not run		Under contact
1061	CC1061-A	2		Not run	
	CC1061-B	2			
	CC1061-D2	2			
	CC1061-D3	2			
	CC1061-D5	1			Above contact
1062	CC1062-1	1			
	CC1062-3	1			
1063	CC1063-2	1			
	CC1063-6	1			

Initial findings

From evaluation of the CT scans and sedimentological observations (fig 3), I hypothesize 5 stratigraphic units within the core (fig 4A). The features of the bottom unit are consistent with a diamicton (unit 1; 2.23-3.44 m depth below the ice-sediment interface), followed by an intermediate ice unit containing few suspended clasts and sediment (unit 2; 1.12-2.23 m). A deformed, normally graded bed of pebbles to silt sized grains (unit 3; 0.89-1.12 m) which overlies unit 2. Above this, we find bedded fine-grained sand (unit 4; 0.56-0.89 m) that coarsens upward into gravelly sand (unit 5; 0-0.56 m).

Diffraction analysis reveals that quartz dominates the mineralogy, followed by plagioclase and feldspar throughout each unit with minimal variability (fig 4B, C). The most variation in the relative mineral distribution occurs near the bottom of unit 2 and the top of unit 1. Here, pyroxenes make up a small, but noticeable, portion of the mineral distribution and one sample contains detectable clay minerals (14Å, Figure 4C).

Micro-scale SEM investigations of grain coatings and shape, like roundness, show more variability throughout the core than the suggested by the mineralogy (fig 5). Grain coatings, possibly glacial flour, are abundant in the lower sections, units 1-3, and almost absent in the two upper-most sections, units 4 and 5. Initial observations indicate that there is not a distinct trend relating to the roundness and circularity of the grains. In part due to the absence of fine grain coatings, there does seem to be more

uniformity in the grain size in the upper units 4 and 5. Whereas in the bottom, especially unit 1, there is more diversity in both size and shape as well as a higher abundance of smaller sized grains.

Synthesizing the mineralogical and sedimentological data, this core shows evidence of a glaciated Greenland followed by at least one period of ice-free conditions. The lower diamicton (unit 1) is likely a glacial till that formed by glacial movement across the landscape. The intermediate ice layer (unit 2) could be a permafrost ice wedge or basal ice from a different glacial advance, but more investigation is necessary to support these hypotheses. Unit 3 has remarkably similar structures to Unit 1. This could mean that they are part of the same unit. The movement and pressure at the base of the glacier entrained what we call unit 3 in the ice, separating it from unit 1. It could also be a slump deposit on top of the lower sediment and was then buried. The upper units are sandy and well sorted in size, transported by fluvial processes, and represent the absence of ice. Unit 4 was deposited in a low energy environment and the uppermost unit (unit 5) shows upward coarsening that indicates a more energetic environment, possibly a meandering stream. Overall, due to the presence of angular grains in these upper units, the energy of the system and transport distance remained low.

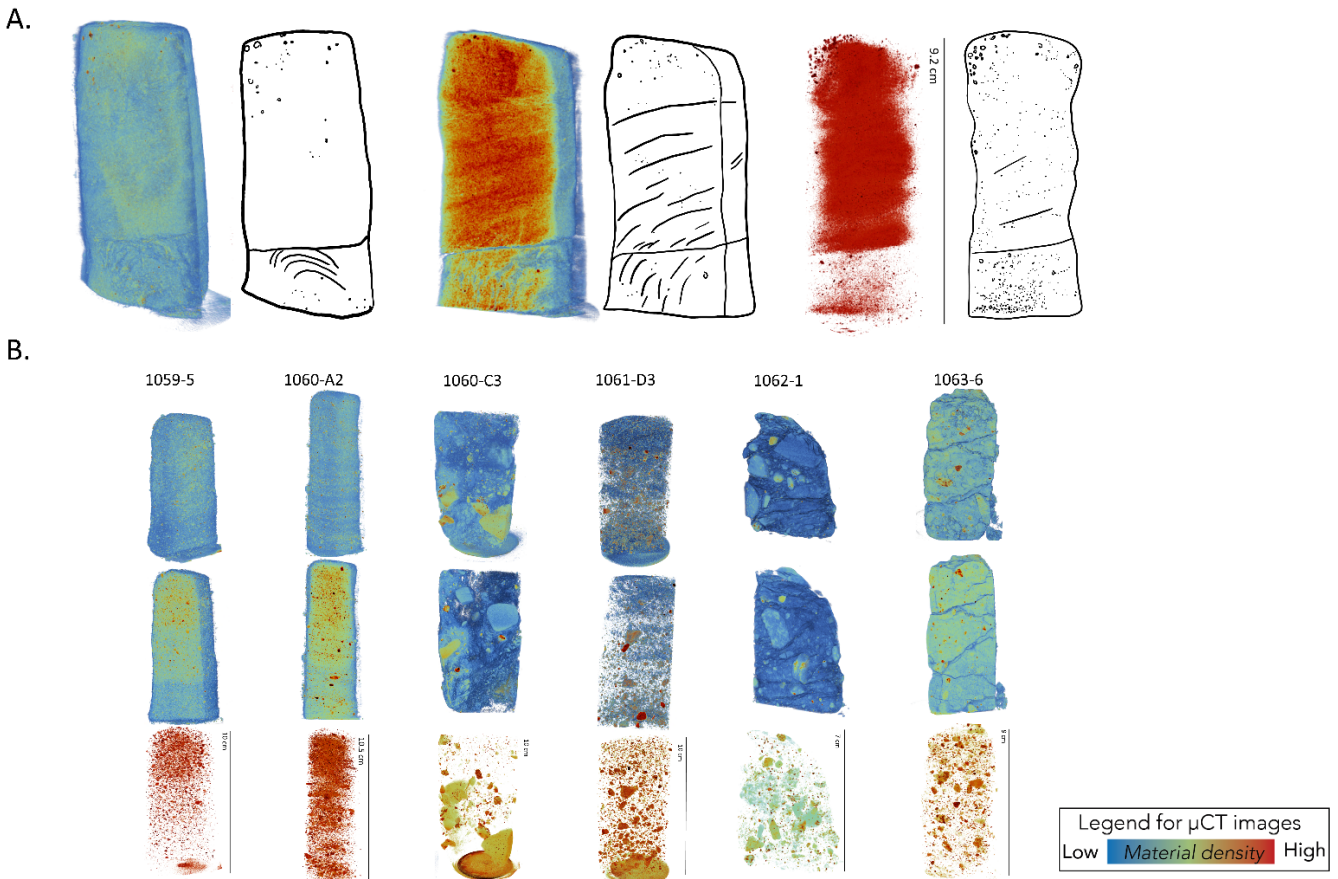


Figure 3 Qualitative data acquisition of core stratigraphy from 3D models of the μ CT scans. (A) Example of macroscale core analysis on a full scan to detect unit contact at the core surface (left) and within the core (middle), supplemented by layering and grain characteristics within the core (right) based on material density. (B) Representative CT scans of subcore samples showing diagnostic features of their hypothesized unit assignments. From top to bottom each sample is shown as a whole (surface view), digitally sliced to access the interior, and the suspended clasts by material density. Samples 1059-5 and 1060-A2 show the coarse grains and linear features characteristic of unit 5. Sample 1060-C3 has a higher ice content and high variation in grain size typical in unit 3. Sample 1061-D3 has a remarkably high ice content and suspended clasts which belongs in unit 2. Samples 1062-1 and 1063-6 both show the variable grain sizes distributed in a fine-grained matrix with abundant ice lenses that is typical of unit 1.

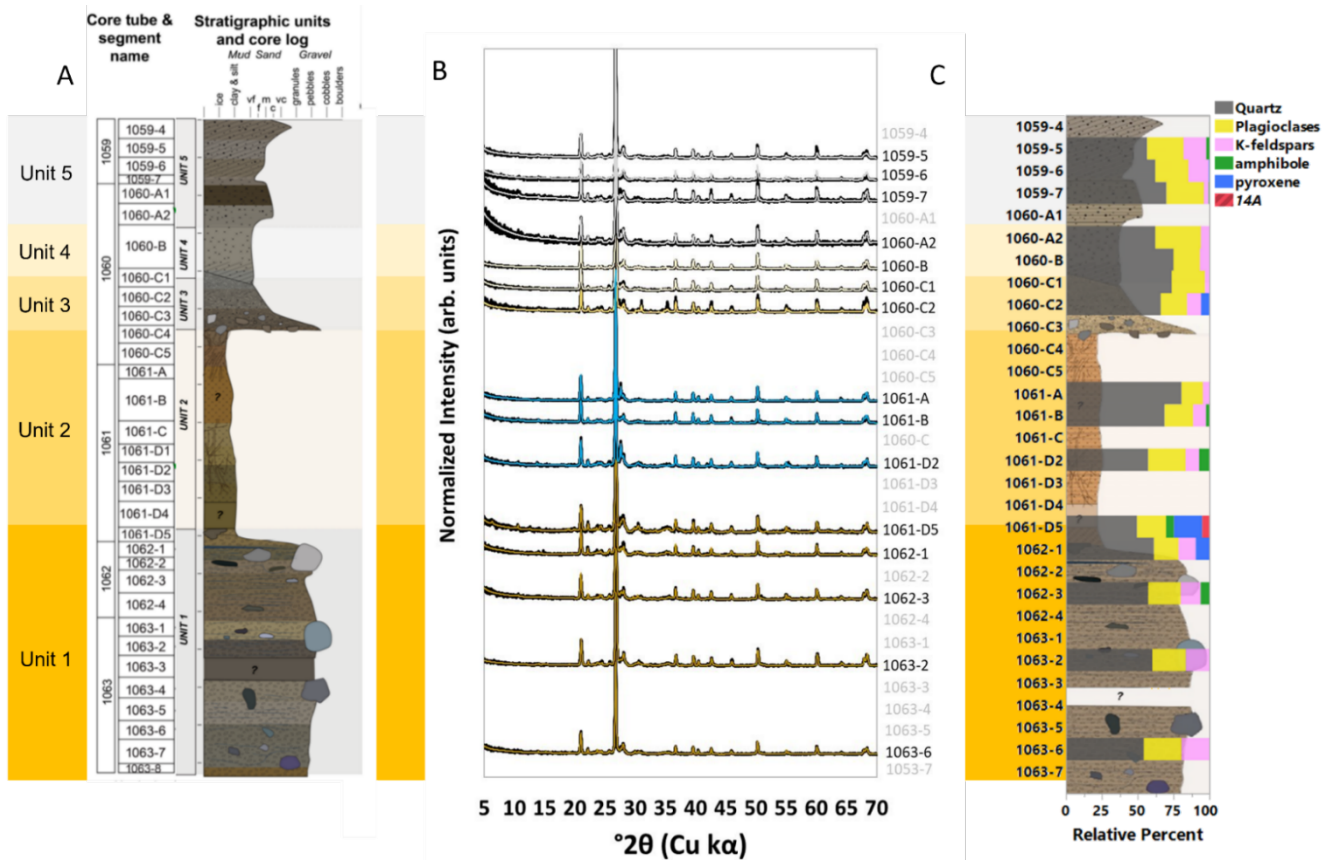


Figure 5. X-Ray Diffraction analysis. (A) depiction of the stratigraphic column, unit distribution, and sample arrangement along the core. (B) Measured (black lines) and modeled (colored lines) diffractograms. (C) Relative percentage of bulk mineralogy from modeled diffractogram over entire core stratigraphic column.

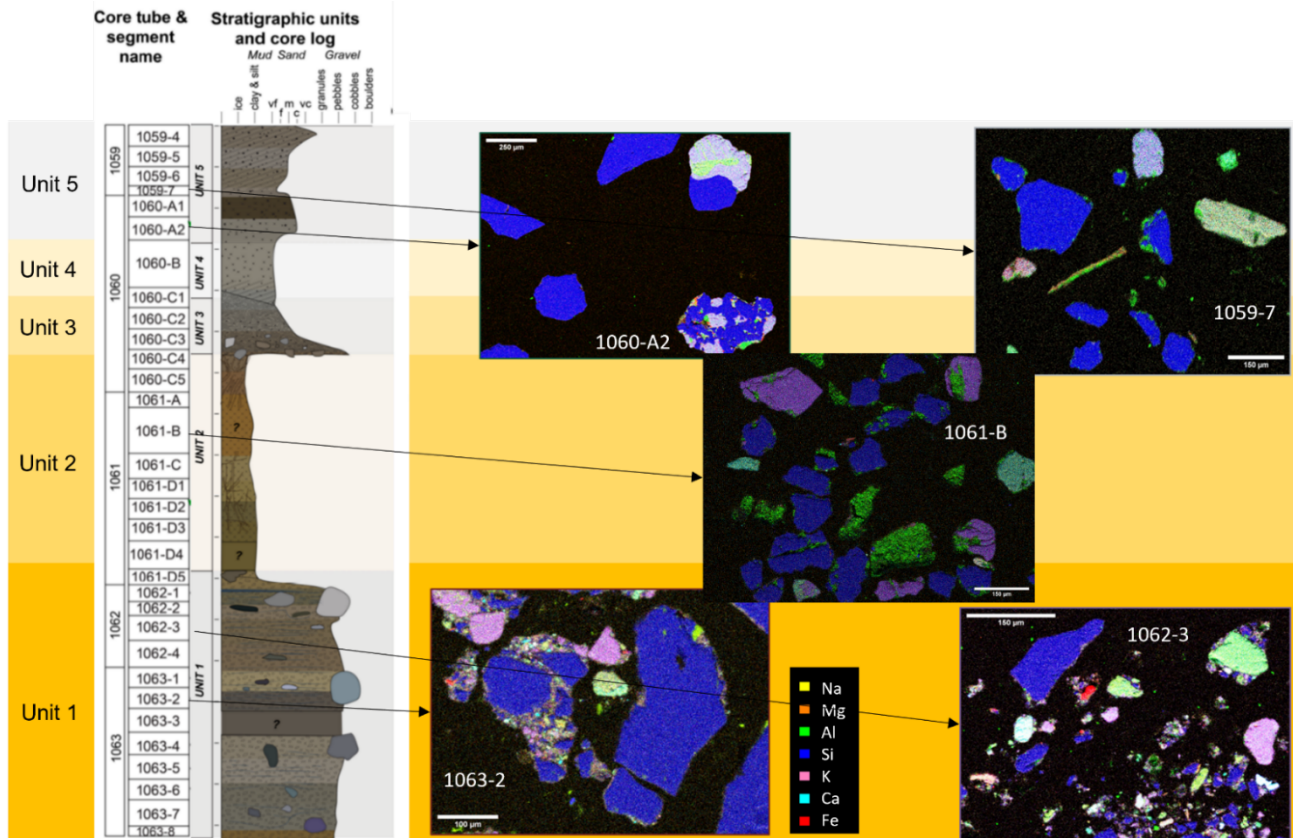


Figure 4. microchemical SEM maps of selected units. Maps are color-coded by element according to the included legend. Note that color blending reflects colocation of elements. For example, while dark blue corresponds to SiO_2 , purple corresponds to a mineral combining Si, Al, and Na, typically a plagioclase.

Future Work

The completion of my thesis requires several efforts. The first is data collection. The outstanding data collection includes quantitative analysis of the CT scans which will include a grain size and grain orientation assessment. There are approximately 100 scans to process which I can automate by batch processing of similar samples in the Bruker CTan software. In addition to this I will finish a grain coating and grain shape analysis using 33 SEM images from 16 samples throughout the core. Compiling this alongside data already available, including the XRD analysis and other analyses done by the mineralogy subgroup in the Camp Century team, I am leading the preparation of a peer-reviewed article aiming at reconstructing the environments of deposition at Camp Century. This manuscript is expected to be submitted to *Cryosphere* in Spring 2024.

Timeline

Timeframe	Goals
Fall 2023	<ul style="list-style-type: none">• Learn to use CT software.• Process scans to extract quantitative data.• Finish SEM scans at Middlebury College• Synthesize 3 data collection methods and how they inform each other.• Start writing mineralogy paper.• Conferences/Workshops:<ul style="list-style-type: none">○ Graduate Climate Conference - Nov○ Ice Core Analysis Techniques - Sept○ AGU – Dec
Spring 2024	<ul style="list-style-type: none">• Continue Data synthesis of 3 methods, include methods from PH and GEUS.• Submission of the manuscript.• Conferences:<ul style="list-style-type: none">○ EGU – Apr
Summer 2024	<ul style="list-style-type: none">• Finish and defend

References

- Bender, M. L., Burgess, E., Alley, R. B., Barnett, B., & Clow, G. D. (2010). On the nature of the dirty ice at the bottom of the GISP2 ice core. *Earth and Planetary Science Letters*, 299(3–4), 466–473. <https://doi.org/10.1016/J.EPSL.2010.09.033>
- Benn, D. I. (2009). Glacial Sediments. In V. Gornitz (Ed.), *Encyclopedia of Paleoclimatology and Ancient Environments* (1st ed.). Springer Dordrecht.
- Bierman, P. R., Corbett, L. B., Graly, J. A., Neumann, T. A., Lini, A., Crosby, B. T., & Rood, D. H. (2014). Preservation of a Preglacial Landscape Under the Center of the Greenland Ice Sheet. *Science*, 344(6182), 402–405. <https://doi.org/10.1126/science.1249047>
- Bierman, P. R., Shakun, J. D., Corbett, L. B., Zimmerman, S. R., & Rood, D. H. (2016). A persistent and dynamic East Greenland Ice Sheet over the past 7.5 million years. *Nature*, 540(7632), 256–260. <https://doi.org/10.1038/nature20147>
- Blard, P. H., Protin, M., Tison, J. L., Fripiat, F., Dahl-Jensen, D., Steffensen, J. P., Mahaney, W. C., Bierman, P. R., Christ, A. J., Corbett, L. B., Debaille, V., Rigaudier, T., & Claeys, P. (2023). Basal debris of the NEEM ice core, Greenland: a window into sub-ice-sheet geology, basal ice processes and ice-sheet oscillations. *Journal of Glaciology*, 268(11). <https://doi.org/10.1017/jog.2022.122>
- Bond, G., Heinrich, H., Broecker, W., Labeyrie, L., McManus, J., Andrews, J., Huon, S., Jantschik, R., Clasen, S., Simet, C., Tedesco, K., Klas, M., Bonani, G., & Ivy, S. (1992). Evidence for massive discharges of icebergs into the North Atlantic ocean during the last glacial period. *Nature*, 360(6401), 245–249. <https://doi.org/10.1038/360245a0>
- Christ, A. J., Bierman, P. R., Schaefer, J. M., Dahl-Jensen, D., Steffensen, J. P., Corbett, L. B., Peteet, D. M., Thomas, E. K., Steig, E. J., Rittenour, T. M., Tison, J.-L., Blard, P.-H., Perdrial, N., Dethier, D. P., Lini, A., Hidy, A. J., Caffee, M. W., & Southon, J. (2021). A multimillion-year-old record of Greenland vegetation and glacial history preserved in sediment beneath 1.4 km of ice at Camp Century. *PNAS*, 118(13), e2021442118. <https://doi.org/10.1073/pnas.2021442118/-/DCSupplemental>
- Christ, A. J., Rittenour, T. M., Bierman, P. R., Keisling, B. A., Knutz, P. C., Thomsen, T. B., Keulen, N., Fosdick, J. C., Hemming, S. R., Tison, J.-L., Blard, P.-H., Steffensen, J. P., Caffee, M. W., Corbett, L. B., Dahl-Jensen, D., Dethier, D. P., Hidy, A. J., Perdrial, N., Peteet, D. M., ... Thomas, E. K. (2023). Deglaciation of northwestern Greenland during Marine Isotope Stage 11. *Science*, 381(6655), 330–335. <https://doi.org/10.1126/science.ade4248>
- Clark, E. F. (1965). *Camp Century Evolution of Concept and History of Design Construction and Performance*.
- de Vernal, A., & Hillaire-Marcel, C. (2008). Natural Variability of Greenland Climate, Vegetation, and Ice Volume During the Past Million Years. *Science*, 320(5883), 1622–1625. <https://doi.org/10.1126/science.1153929>
- Dutton, A., Carlson, A. E., Long, A. J., Milne, G. A., Clark, P. U., DeConto, R., Horton, B. P., Rahmstorf, S., & Raymo, M. E. (2015). Sea-level rise due to polar ice-sheet mass loss during past warm periods. *Science*, 349(6244). <https://doi.org/10.1126/science.aaa4019>

- Evans, D. J. A., Phillips, E. R., Hiemstra, J. F., & Auton, C. A. (2006). Subglacial till: Formation, sedimentary characteristics and classification. *Earth-Science Reviews*, 78(1–2), 115–176. <https://doi.org/10.1016/j.earscirev.2006.04.001>
- Finkel, R. C., & Nishiizumi, K. (1997). Beryllium 10 concentrations in the Greenland Ice Sheet Project 2 ice core from 3–40 ka. *Journal of Geophysical Research: Oceans*, 102(C12), 26699–26706. <https://doi.org/10.1029/97JC01282>
- Fountain, J., Usselman, T. M., Wooden, J., & Langway, C. C. (1981). Evidence of the Bedrock Beneath the Greenland Ice Sheet Near Camp Century, Greenland. *Journal of Glaciology*, 27(95), 193–197. <https://doi.org/10.3189/S0022143000011370>
- French, H., & Shur, Y. (2010). The principles of cryostratigraphy. *Earth-Science Reviews*, 101(3–4), 190–206. <https://doi.org/10.1016/j.earscirev.2010.04.002>
- Gow, A. J., & Meese, D. A. (1996). Nature of basal debris in the GISP2 and Byrd ice cores and its relevance to bed processes. *Annals of Glaciology*, 22, 134–140. <https://doi.org/10.3189/1996AoG22-1-134-140>
- Grootes, P. M., Stuiver, M., White, J. W. C., Johnsen, S., & Jouzel, J. (1993). Comparison of oxygen isotope records from the GISP2 and GRIP Greenland ice cores. *Nature*, 366(6455), 552–554. <https://doi.org/10.1038/366552a0>
- Grousset, F. E., Labeyrie, L., Sinko, J. A., Cremer, M., Bond, G., Duprat, J., Cortijo, E., & Huon, S. (1993). Patterns of Ice-Rafted Detritus in the Glacial North Atlantic (40–55°N). *Paleoceanography*, 8(2), 175–192. <https://doi.org/10.1029/92PA02923>
- Hansen, B. L., & Langway, C. C. (1966a). Deep Core Drilling in Ice and Core Analysis at Camp Century, Greenland, 1961–1966. *Antarctic Journal of the United States*, 1(5), 207–208.
- Hansen, B. L., & Langway, C. C. (1966b). *Glaciology Deep Core Drilling in Ice and Core Analysis at Camp Century, Greenland, 1961–1966*.
- Harwood, D. M. (1986). Do Diatoms beneath the Greenland Ice Sheet Indicate Interglacials Warmer than Present? *Arctic*, 39(4), 304–308.
- Johnsen, S. J., Dahl-Jensen, D., Gundestrup, N., Steffensen, J. P., Clausen, H. B., Miller, H., Masson-Delmotte, V., Sveinbjörnsdóttir, A. E., & White, J. (2001). Oxygen isotope and palaeotemperature records from six Greenland ice-core stations: Camp Century, Dye-3, GRIP, GISP2, Renland and NorthGRIP. *Journal of Quaternary Science*, 16(4), 299–307. <https://doi.org/10.1002/JQS.622>
- Johnsen, S. J., Dansgaard, W., Clausen, H. B., & Lang Way, C. C. (1972). Oxygen Isotope Profiles through the Antarctic and Greenland Ice Sheets. In *Biochem. Biophys. Res. Commun* (Vol. 235).
- Johnson, T. C. (1981). Origin of sedimentary rocks (Second edn.), H. Blatt, G. Middleton, and R. Murray, Prentice-Hall, Inc., 1980. *Earth Surface Processes and Landforms*, 6(1). <https://doi.org/10.1002/esp.3290060115>
- Jouzel, J., Masson-Delmotte, V., Cattani, O., Dreyfus, G., Falourd, S., Hoffmann, G., Minster, B., Nouet, J., Barnola, J. M., Chappellaz, J., Fischer, H., Gallet, J. C., Johnsen, S., Leuenberger, M., Loulergue, L., Luethi, D., Oerter, H., Parrenin, F., Raisbeck, G., ... Wolff, E. W. (2007). Orbital and Millennial

- Antarctic Climate Variability over the Past 800,000 Years. *Science*, 317(5839), 793–796. <https://doi.org/10.1126/science.1141038>
- Knight, P. G. (1997). The basal ice layer of glaciers and ice sheets. *Quaternary Science Reviews*, 16(9), 975–993. [https://doi.org/10.1016/S0277-3791\(97\)00033-4](https://doi.org/10.1016/S0277-3791(97)00033-4)
- Kukla, G., McManus, J. F., Rousseau, D. D., & Chuine, I. (1997). How long and how stable was the last interglacial? *Quaternary Science Reviews*, 16(6), 605–612. [https://doi.org/10.1016/S0277-3791\(96\)00114-X](https://doi.org/10.1016/S0277-3791(96)00114-X)
- Langway, C. C. (2008). The History of Early Polar Ice Cores. *Cold Regions Science and Technology*, 52(2), 101–117. <https://doi.org/10.1016/j.coldregions.2008.01.001>.
- Langway, C. C., & Hansen, B. L. (1970). Drilling Through the Ice Cap: Probing Climate for a Thousand Centuries. *Bulletin of the Atomic Scientists*, 26(10), 62–66.
- Lisiecki, L. E., & Raymo, M. E. (2005). A Pliocene-Pleistocene stack of 57 globally distributed benthic $\delta^{18}O$ records. *Paleoceanography*, 20(1), 1–17. <https://doi.org/10.1029/2004PA001071>
- Loutre, M. F., & Berger, A. (2003). Marine Isotope Stage 11 as an analogue for the present interglacial. *Global and Planetary Change*, 36(3), 209–217. [https://doi.org/10.1016/S0921-8181\(02\)00186-8](https://doi.org/10.1016/S0921-8181(02)00186-8)
- Lüthi, D., Le Floch, M., Bereiter, B., Blunier, T., Barnola, J.-M., Siegenthaler, U., Raynaud, D., Jouzel, J., Fischer, H., Kawamura, K., & Stocker, T. F. (2008). High-resolution carbon dioxide concentration record 650,000–800,000 years before present. *Nature*, 453(7193), 379–382. <https://doi.org/10.1038/nature06949>
- Mahaney, W. C. (2011). SEM Analysis of Glacial Sediments. In V. P. Singh, P. Singh, & U. K. Haritashya (Eds.), *Encyclopedia of Snow, Ice and Glaciers* (1st ed.). Springer Science. https://doi.org/10.1007/978-90-481-2642-2_651
- Manabe, S., & Stouffer, R. J. (1980). Sensitivity of a global climate model to an increase of CO₂ concentration in the atmosphere. *Journal of Geophysical Research*, 85(C10), 5529. <https://doi.org/10.1029/JC085iC10p05529>
- Meyer, H., Dereviagin, A., Siebert, C., Schirrmeister, L., & Hubberten, H.-W. (2002). Palaeoclimate reconstruction on Big Lyakhovsky Island, north Siberia-hydrogen and oxygen isotopes in ice wedges. *Permafrost and Periglacial Processes*, 13(2), 91–105. <https://doi.org/10.1002/ppp.416>
- Murton, J. B., & French, H. M. (1994). Cryostructures in permafrost, Tuktoyaktuk coastlands, western arctic Canada. *Canadian Journal of Earth Sciences*, 31(4), 737–747. <https://doi.org/10.1139/e94-067>
- Preibisch, S., Saalfeld, S., & Tomancak, P. (2009). Globally optimal stitching of tiled 3D microscopic image acquisitions. *Bioinformatics*, 25(11), 1463–1465. <https://doi.org/10.1093/bioinformatics/btp184>
- Rantanen, M., Karpechko, A. Yu., Lipponen, A., Nordling, K., Hyvärinen, O., Ruosteenoja, K., Vihma, T., & Laaksonen, A. (2022). The Arctic has warmed nearly four times faster than the globe since 1979. *Communications Earth & Environment*, 3(1), 168. <https://doi.org/10.1038/s43247-022-00498-3>

- Rentschler, J., Salhab, M., & Jafino, B. A. (2022). Flood exposure and poverty in 188 countries. *Nature Communications*, *13*(1), 3527. <https://doi.org/10.1038/s41467-022-30727-4>
- Reyes, A. V., Carlson, A. E., Beard, B. L., Hatfield, R. G., Stoner, J. S., Winsor, K., Welke, B., & Ullman, D. J. (2014a). South Greenland ice-sheet collapse during Marine Isotope Stage 11. *Nature*. <https://doi.org/10.1038/nature13456>
- Reyes, A. V., Carlson, A. E., Beard, B. L., Hatfield, R. G., Stoner, J. S., Winsor, K., Welke, B., & Ullman, D. J. (2014b). South Greenland ice-sheet collapse during Marine Isotope Stage 11. *Nature*, *510*(7506), 525–528. <https://doi.org/10.1038/nature13456>
- Rietveld, H. M. (1969). A profile refinement method for nuclear and magnetic structures. *Journal of Applied Crystallography*, *2*(2), 65–71. <https://doi.org/10.1107/S0021889869006558>
- Schaefer, J. M., Finkel, R. C., Balco, G., Alley, R. B., Caffee, M. W., Briner, J. P., Young, N. E., Gow, A. J., & Schwartz, R. (2016). Greenland was nearly ice-free for extended periods during the Pleistocene. *Nature*, *540*(7632), 252–255. <https://doi.org/10.1038/nature20146>
- Schindelin, J., Arganda-Carreras, I., Frise, E., Kaynig, V., Longair, M., Pietzsch, T., Preibisch, S., Rueden, C., Saalfeld, S., Schmid, B., Tinevez, J.-Y., White, D. J., Hartenstein, V., Eliceiri, K., Tomancak, P., & Cardona, A. (2012). Fiji: an open-source platform for biological-image analysis. *Nature Methods*, *9*(7), 676–682. <https://doi.org/10.1038/nmeth.2019>
- Schindler, M., & Singer, D. M. (2017). Mineral surface coatings: Environmental records at the nanoscale. *Elements*, *13*(3), 159–164. <https://doi.org/10.2113/gselements.13.3.159>
- Smith, B., Fricker, H. A., Gardner, A. S., Medley, B., Nilsson, J., Paolo, F. S., Holschuh, N., Adusumilli, S., Brunt, K., Csatho, B., Harbeck, K., Markus, T., Neumann, T., Siegfried, M. R., & Zwally, H. J. (2020). *Pervasive ice sheet mass loss reflects competing ocean and atmosphere processes*. <https://doi.org/10.1126/science.aaz5845>
- Souchez, R., Bouzette, A., Clausen, H. B., Johnsen, S. J., & Jouzel, J. (1998). A stacked mixing sequence at the base of the Dye 3 core, Greenland. *Geophysical Research Letters*, *25*(10), 1943–1946. <https://doi.org/10.1029/98gl01411>
- Souchez, R., Janssens, L., Lemmens, M., & Stauffer, B. (1995). Very low oxygen concentration in basal ice from Summit, central Greenland. *Geophysical Research Letters*, *22*(15), 2001–2004. <https://doi.org/10.1029/95GL01995>
- Souchez, R., Jouzel, J., Landais, A., Chappellaz, J., Lorrain, R., & Tison, J. L. (2006). Gas isotopes in ice reveal a vegetated central Greenland during ice sheet invasion. *Geophysical Research Letters*, *33*(24). <https://doi.org/10.1029/2006GL028424>
- Souchez, R., Lemmens, M., & Chappellaz, J. (1995). *Flow-induced mixing in the GRIP basal ice deduced from the CO₂ and CH₄ records* (Vol. 22, Issue 1).
- Souchez, R., Tison, J. -L., Lorrain, R., Lemmens, M., Janssens, L., Stievenard, M., Jouzel, J., Sveinbjörnsdóttir, A., & Johnsen, S. J. (1994). Stable isotopes in the basal silty ice preserved in the Greenland Ice Sheet at summit; environmental implications. *Geophysical Research Letters*, *21*(8), 693–696. <https://doi.org/10.1029/94GL00641>

- Suwa, M., von Fischer, J. C., Bender, M. L., Landais, A., & Brook, E. J. (2006). Chronology reconstruction for the disturbed bottom section of the GISP2 and the GRIP ice cores: Implications for Termination II in Greenland. *Journal of Geophysical Research: Atmospheres*, *111*(D2), 2101. <https://doi.org/10.1029/2005JD006032>
- Svensson, A., Bigler, M., Kettner, E., Dahl-Jensen, D., Johnsen, S., Kipfstuhl, S., Nielsen, M., & Steffensen, J. P. (2011). Annual layering in the NGRIP ice core during the Eemian. *Climate of the Past*, *7*(4), 1427–1437. <https://doi.org/10.5194/CP-7-1427-2011>
- Taylor, K. C., Hammer, C. U., Alley, R. B., Clausen, H. B., Dahl-Jensen, D., Gow, A. J., Gundestrup, N. S., Kipfstuhl, J., Moore, J. C., & Waddington, E. D. (1993). Electrical conductivity measurements from the GISP2 and GRIP Greenland ice cores. *Nature*, *366*(6455), 549–552. <https://doi.org/10.1038/366549a0>
- Tison, J.-L., Blard, P.-H., Wauthy, S., Protin, M., & Ardoin, L. (2019). A Census of Basal Ice Samples from Deep Ice Cores at NBI. *Oldest Ice of Greenland - Workshop at University of Vermont*, *299*(3–4). <https://cnrs.hal.science/hal-03420093>
- Velde, B. (1995). Geology of Clays. In *Origin and Mineralogy of Clays* (pp. 1–7). Springer Berlin Heidelberg. https://doi.org/10.1007/978-3-662-12648-6_1
- W. Dansgaard, S. J. Johnsen, J. Moller, & C. C. Langway Jr. (1969). One Thousand Centuries of Climatic Record from Camp Century on the Greenland Ice Sheet. *Science*.
- Whalley, W. B., & Langway, C. C. (1980). A Scanning Electron Microscope Examination of Subglacial Quartz Grains from Camp Century Core, Greenland—A Preliminary Study. *Journal of Glaciology*, *25*(91), 125–132. <https://doi.org/10.3189/s0022143000010340>
- Willerslev, E., Cappellini, E., Boomsma, W., Nielsen, R., Hebsgaard, M. B., Brand, T. B., Hofreiter, M., Bunce, M., Poinar, H. N., Dahl-Jensen, D., Johnsen, S., Steffensen, J. P., Bennike, O., Schwenninger, J. L., Nathan, R., Armitage, S., De Hoog, C. J., Alfimov, V., Christl, M., ... Collins, M. J. (2007). Ancient biomolecules from deep ice cores reveal a forested southern Greenland. *Science*, *317*(5834), 111–114. https://doi.org/10.1126/SCIENCE.1141758/SUPPL_FILE/WILLERSLEV.SOM.REVISION.1.PDF
- Willerslev, E., Cappellini, E., Boomsma, W., Nielsen, R., Hebsgaard, M. B., Brand, T. B., Hofreiter, M., Bunce, M., Poinar, H. N., Dahl-Jensen, D., Johnsen, S., Steffensen, J. P., Bennike, O., Schwenninger, J.-L., Nathan, R., Armitage, S., de Hoog, C.-J., Alfimov, V., Christl, M., ... Collins, M. J. (2007). Ancient Biomolecules from Deep Ice Cores Reveal a Forested Southern Greenland. *Science*, *317*(5834), 111–114. <https://doi.org/10.1126/science.1141758>
- Yau, A. M., Bender, M. L., Blunier, T., & Jouzel, J. (2016). Setting a chronology for the basal ice at Dye-3 and GRIP: Implications for the long-term stability of the Greenland Ice Sheet. *Earth and Planetary Science Letters*, *451*, 1–9. <https://doi.org/10.1016/J.EPSL.2016.06.053>
- Young, G. M. (2016). Ice ages in earth history: Puzzling paleolatitudes and regional provenance of ice sheets on an evolving planet. In *Sediment Provenance: Influences on Compositional Change from Source to Sink* (pp. 533–562). Elsevier. <https://doi.org/10.1016/B978-0-12-803386-9.00019-8>